PERGAMON International Journal of Impact Engineering 25 (2001) 927–947

INTERNATIONAL JOURNAL OF IMPACT ENGINEERING

www.elsevier.com/locate/ijimpeng

Experimental and computational analysis of plates under air blast loading

Abel Carlos Jacinto[a], Ricardo Daniel Ambrosini[b,*], Rodolfo Francisco Danesi[c]

[a] *Structures Laboratory, National University of Tucuman, Argentina Lamadrid 782 1 D. 4000 San Miguel de Tucumán, Tucumán, Argentina*

[b] *Structures Laboratory, National University of Tucumán, CONICET, Argentina Lola Mora 380, 4000 San Miguel de Tucumán, Tucumán, Argentina*

[c] *Structures Laboratory, National University of Tucumán, CONICET, Argentina. Muñecas 586 1 A. 4000 San Miguel de Tucumán, Tucumán, Argentina*

Received 29 August 2000; received in revised form 12 April 2001; accepted 15 June 2001

Abstract

The main objective of this paper is the comparison between testing and numerical responses of metallic plates subjected to explosive loads, in order to obtain guides to the numerical modeling and analysis of this phenomenon. Moreover, the secondary objective was to provide data that could be used for checking the accuracy of a variety of calculation methods. A set of four tests at natural scale is presented on two nonstiffened metallic steel plates with different boundary conditions (one clamped in the soil and another clamped in the four edges), subjected to the action of pressure waves originated by the detonation of explosive loads. The time history of the acceleration in different points of both plates and the pressure waves in selected points, are recorded. On the other hand, a linear dynamic analysis of the plate models with the code ABAQUS was carried out. The influence of the number of natural modes that are considered for the analysis and the refinement of the mesh are analyzed. Moreover, a nonlinear geometric analysis was carried out in order to verify this possible behavior in the first plate. Suggestions to computational modeling of structures under impulsive loads arise from the comparison of numerical and experimental results.

Keywords: Air blast waves; Unstiffened plates; Dynamic response; Experimental analysis

*Corresponding author. Tel.: +54-381-436-4087; fax: +54-381-436-4087.
E-mail address: dambrosini@herrera.unt.edu.ar (R.D. Ambrosini).

0734-743X/01/$ - see front matter
PII: S0734-743X(01)00031-8

1. Introduction

In recent years, the explosive loads have received considerable attention by different events, accidental or intentional, over important structures all over the world. In consequence, in the last decade there was an important activity in the research of explosive loads. Initially, these works were mostly empirical, but, in the last few years, important researches have begun to develop.

The detonation of an explosive generates the violent expansion of hot gases originating a pressure wave, moving outward at high velocity from its source. When the front of the shock wave arrives at the observation point the pressure rises very sharply, followed by a quasi exponential decay back to ambient pressure p_o and a negative phase in which the pressure is less than ambient. The peak values of the underpressure are usually small compared with the peak positive overpressure. When the shock wave arrives at a point of interest it originates a dynamic pressure that is proportional to the square of the wind velocity and the density of the air behind the shock front. Finally, when the incident blast wave from an explosion in air strikes a more dense medium (earth, water, wall), it is reflected. The peak value of the reflected pressure depends on the peak of the incident wave, the angle at which it strikes the surface and the nature of the surface.

Generally, simplifying assumptions must be made in order to solve specific problems. Until now, most practical problems have been solved through empirical approaches. Years of industrial and military experience have been condensed in charts or equations [1,2]. In connection with structural analysis there are several simple methods in the classical books of structural dynamics by Biggs [3] and Clough and Penzien [4]. For a more rigorous analysis, the structure model as a system of multiple degree of freedom and the equilibrium equation solves using modal superposition or direct integration methods. If the difference exists between the stiffness of the component parts of the structure (resistant structure and panels), then it is possible to separate them. In this case, the parts can be analyzed in separate ways [5].

The dynamic loads originated by explosions are impulsive and result in strain rates in the material about 10^{-1}–$10^{3}\,\mathrm{seg}^{-1}$. These extreme loads produce a special behavior in the material that is characterized, among other effects, by overstrength and increased stiffness, in comparison with normal, static properties. Galiev [6] and Krauthammer et al. [7] describe the metal behavior under impulsive load.

In the analysis, it is sometimes necessary to consider the effects of geometric and material nonlinearities. Louca et al. [8] propose a method based on Lagrange equation to realize an elastic analysis considering large displacement. Theoretical analysis considers only simple boundary conditions, while modeling of other boundary conditions is possible using springs. Ellis and Tsui [9] indicate a method to determine the stiffness of spring. Many papers using the plastic hinged model were proposed by Jones [10]. In the paper of Nonaka [11], attention is focused on the failure mode of a steel brace in New York World Trade Center.

In connection with tests it is usual to refer the weight of used explosives to an equivalent weight of TNT. The results presented by Formby and Wharton [12] are very useful to understand and to obtain the TNT equivalence of various commercial explosives.

The objectives of this paper are, first, the comparison between testing and numerical responses in order to obtain guides to the numerical modeling and analysis of this phenomenon and, in the second place, to provide data that could be used for checking the accuracy of a variety of

calculation methods. According to these objectives, a set of four tests at natural scale was performed on two unstiffened metallic steel plates with different boundary conditions (one clamped in the soil and another clamped in the four edges), subjected to the action of pressure waves originated by the detonation of explosive loads. The time history of the acceleration in different points of both plates and the pressure waves in selected points, are recorded. On the other hand, a numerical analysis using the finite element program ABAQUS/Standard [13] was carried out. At first, a linear dynamic analysis considering small displacements was performed and afterwards a nonlinear dynamic analysis considering large displacements was executed. Related with this research, Ellis et al. [9] present experimental results of reinforced concrete panels subjected to explosive loading; Rudrapatna et al. [14] present numerical results for clamped, square stiffened steel plates subjected to blast loading and Louca et al. [8] describe numerical results of nonlinear analysis on both stiffened and unstiffened plates. On the other hand, Shen and Jones [15] analyse the nonlinear dynamic response and failure of clamped circular plates.

The results presented in this paper could be used in order to obtain design guidelines of offshore topsides and steel bridge plated construction. In connection with this, Pan and Louca [16] said that while there has been interest in blast resistance of plates and panels over the past few years, there is very little data available on their response characteristics. Moreover, some aspects are useful for the verification of vehicle barrier systems used to prevent the intrusion of malevolent vehicles with explosives in nuclear power plants (NUREG/CR-6190 [17]). These barriers are designed to resist the kinetic energy of the vehicle and can be verified to the subsequent explosion.

2. Experimental study

2.1. Experimental setup and instrumentation

The analyzed structures in this paper are two unstiffened steel plates subject to impulsive loads originated by detonation of explosives. The explosive used was Gelamon VF80 theoretically equivalent in mass to 80% TNT. This explosive is similar to Special Gelatine 80 (Formby and Wharton [12]). Four tests with different amounts of explosives were carried out (Fig. 1). In order to measure the overpressure generated by the shock waves, four pressure sensors Honeywell 180PC were used (Fig. 2). On the other hand, three accelerometers KYOWA AS-GB were used to measure the dynamic response of the plates (Fig. 3). A dynamic strain amplifier KYOWA DPM-612B amplified the signal generated by the accelerometers. A data acquisition board Computerboars PCM-DAS16D/16 of 100 KHz was mounted on a notebook computer in order to record and process the signals by means of the program HP VEE 5.0. A scheme of the equipment is presented in Fig. 4. Seven channels were used in all tests and the signals were sampled at 4000 Hz for each channel.

The experimental time-history of pressure was used as external load in the computational analysis of the plates. A typical pressure-time history is given in Fig. 5, corresponding to Test 2. A photograph of the test setup is given in Fig. 6 in which the accelerometers and pressure transducers are positioned.

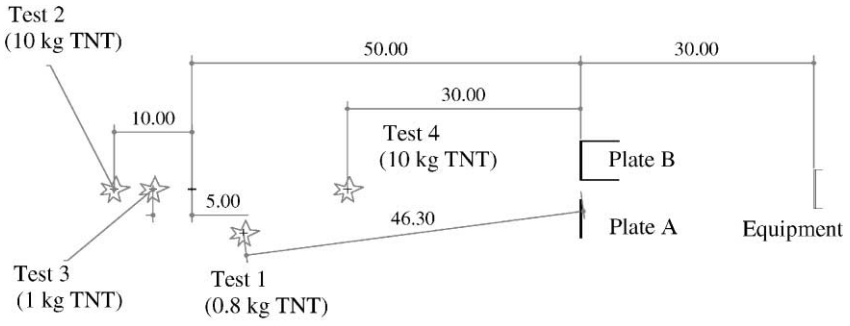

Fig. 1. Experimental setup (distances in m).

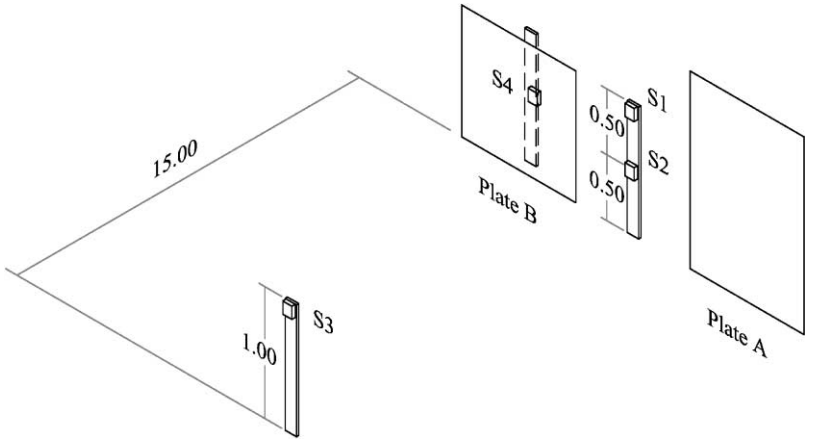

Fig. 2. Pressure sensor locations (distances in m).

2.2. Metallic plate clamped in the bottom (Plate A)

The steel plate A has dimensions 1.0×1.5 m and 2.1 mm of thickness. The bottom of the plate was clamped to a concrete base (Fig. 3). The accelerometer locations in the tests are shown in Fig. 3 that, for the case of Test 1, were positioned in the points 1 and 2. The experimental dynamic response measured for Tests 1, 2 and 4 are presented in Section 4.

2.3. Metallic plate clamped in the four edges (Plate B)

The steel plate B has dimensions 0.95×0.95 m and 0.9 mm of thickness. The four edges of the plate were subjected to a rigid frame of INP 100. This frame was clamped at concrete bases

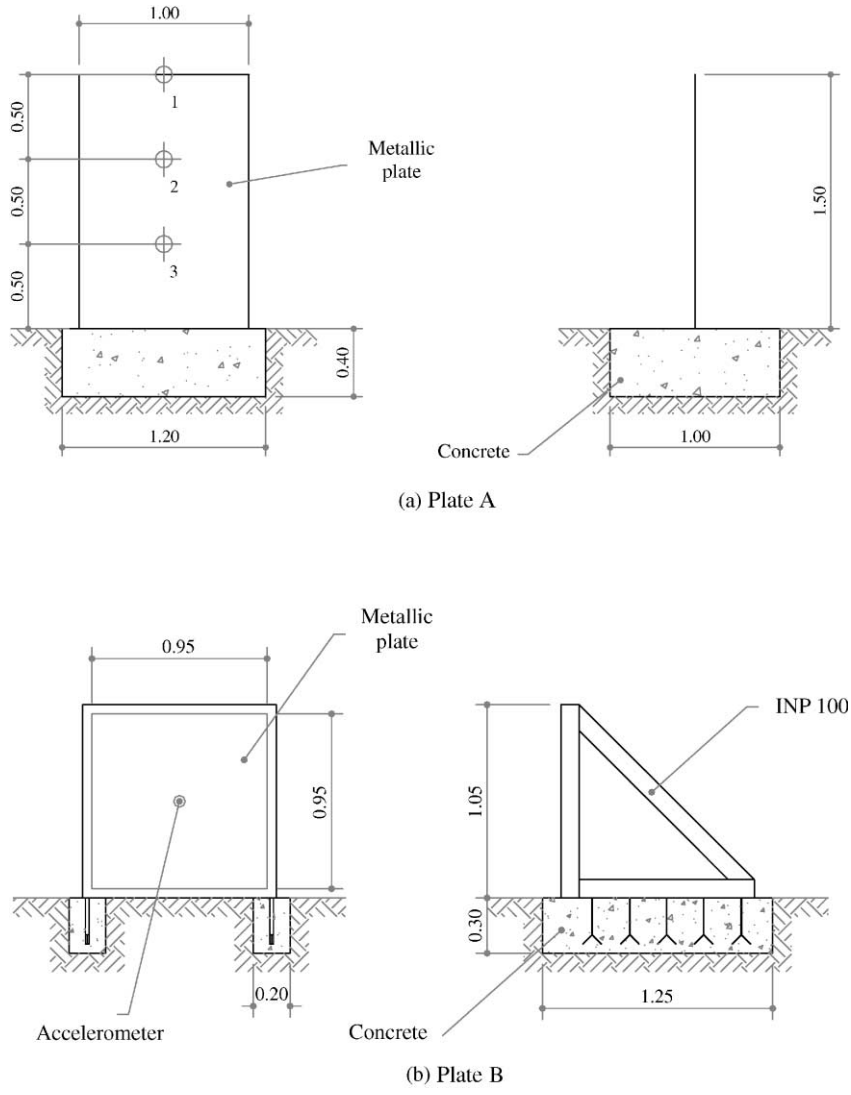

Fig. 3. Scheme of the plates (distances in m).

(Fig. 3). The accelerometer was located in the center of the plate (Fig. 3). Due to the large accelerations involved only the experimental dynamic response measured for Test 1 is presented in Section 4.

2.4. Determination of damping

Based on the acceleration response of the plates, the equivalent viscous-damping ratio was estimated based on the exponential decaying method (Clough and Penzien [4]) and the results are

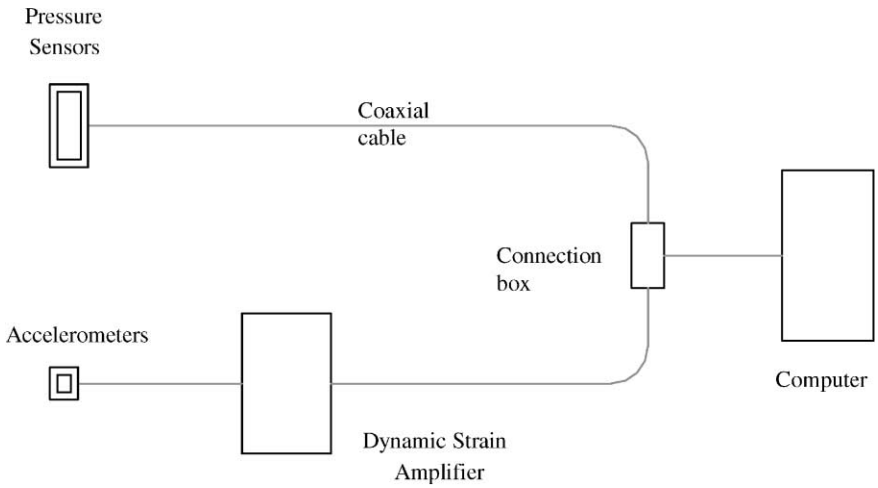

Fig. 4. Scheme of the equipment.

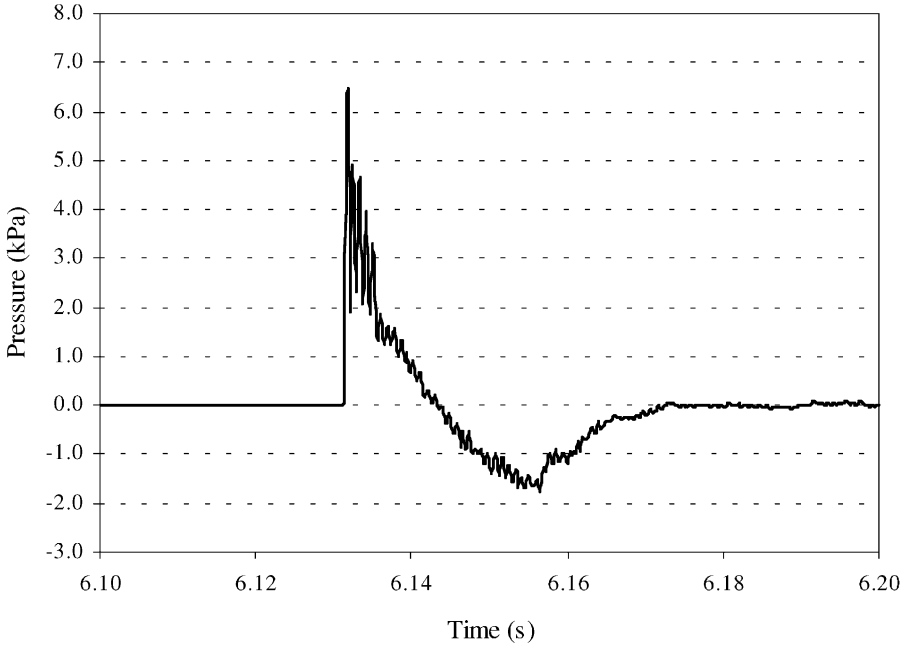

Fig. 5. Record of the time history of the overpressure.

presented in Table 1. Many determinations were performed for both plates on various tests in order to obtain more reliable results.

The difference between the damping of both plates can be explained by the "boundary damping" in the plate-frame union. When damping is measured on a built-up structure, it is commonly found to be at least an order of magnitude higher than the intrinsic material damping

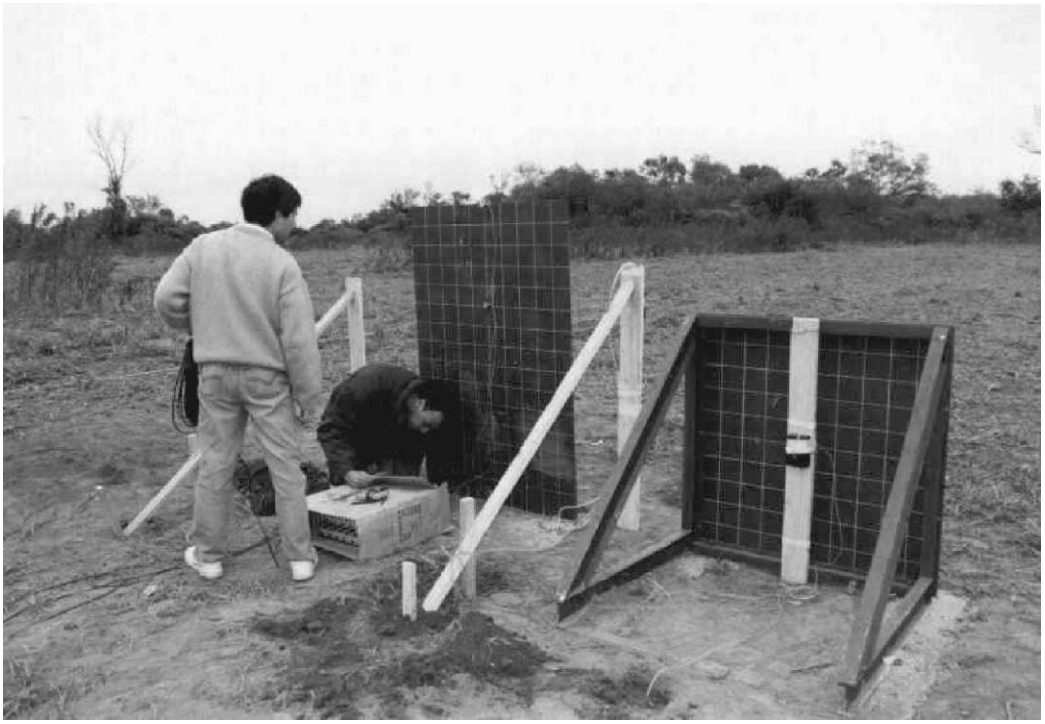

Fig. 6. Arrangement of the plates.

Table 1
Viscous-damping ratios

Damping ratio	Plate A	Plate B
Mean (%)	0.6	2.2
Standard deviation	0.0015	0.0049
Coefficient of variation (%)	25	22

of the main components of the structure. This difference is due to effects such as frictional micro-slipping at joints, air-pumping in riveted seams, etc. (Woodhouse [18]).

3. Numerical analysis

The numerical analysis was carried out using the finite element program ABAQUS/Standard 5.7. The plates were modeled using shell elements. In both cases, the boundary conditions were considered as perfectly clamped. The adopted material properties were Young modulus $E = 180\,\text{GPa}$ (experimental value), Poisson's coefficient $\nu = 0.3$ and density $\rho = 7850\,\text{kg/m}^3$. The dynamic analysis was performed using the modal superposition method and integration

direct method. The integration was carried out step by step using the Newmark-β method ($\beta = \frac{1}{4}$ and $\gamma = \frac{1}{2}$) and the time step size was 0.25 ms. The time-history of the acceleration in the nodes corresponding to the accelerometer position in the test was determined.

3.1. Metallic plate clamped in the bottom (Plate A)

Model 1 of Plate A is formed by 150 elements (10×15 mesh). Furthermore, *Model 2* of 600 elements (20×30 mesh) was used to determine the influence of the refinement of the mesh in the results. The adopted damping coefficient was 0.6%. This value, obtained experimentally as indicated in 2.4, is similar to other values found in the literature for steel.

3.1.1. External action

The time-history of the pressure shown in Fig. 7 was used as external load for the numerical analysis. This curve was obtained for the overlapping in the time of the recorded pressure in Sensor 2 (front) and Sensor 4 (back), according to Fig. 2. In order to introduce a "soft" variation in the input pressure, the oscillations observed in the positive phase of the shock wave were smoothing, considering only the upper points of the curve.

3.1.2. Dynamic response

At first, the modal superposition method was used in the analysis, considering 30 modes. The time history of the accelerations, obtained with ABAQUS, for models 1 and 2 are shown in Fig. 8

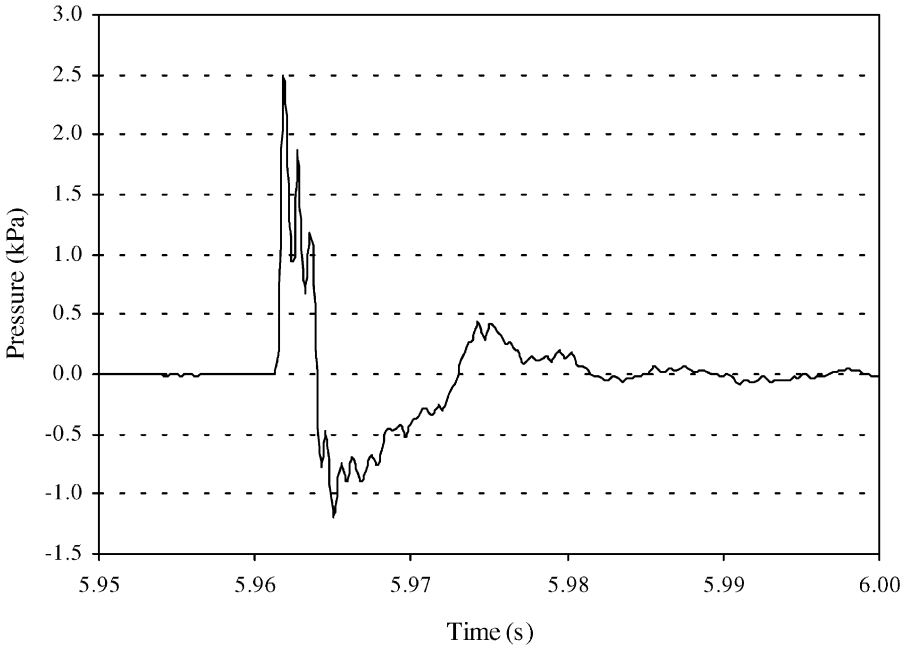

Fig. 7. External load used in the analysis.

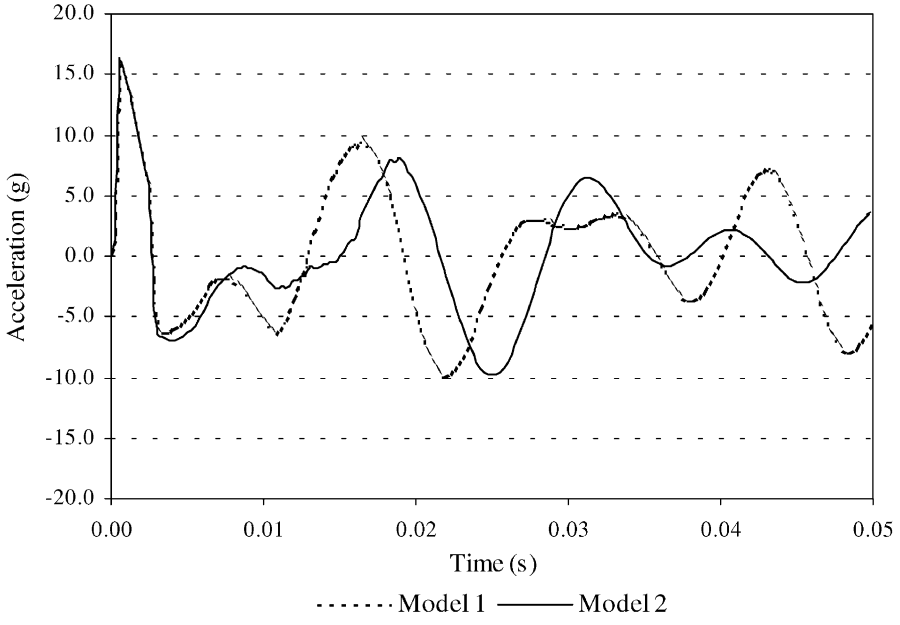

(a) Position 1

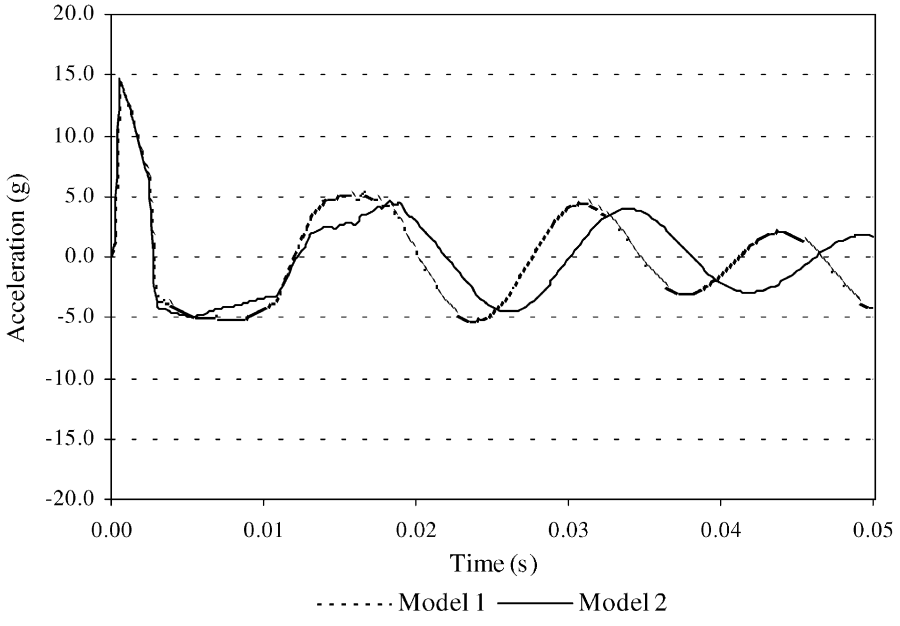

(b) Position 2

Fig. 8. Numerical response. Plate A.

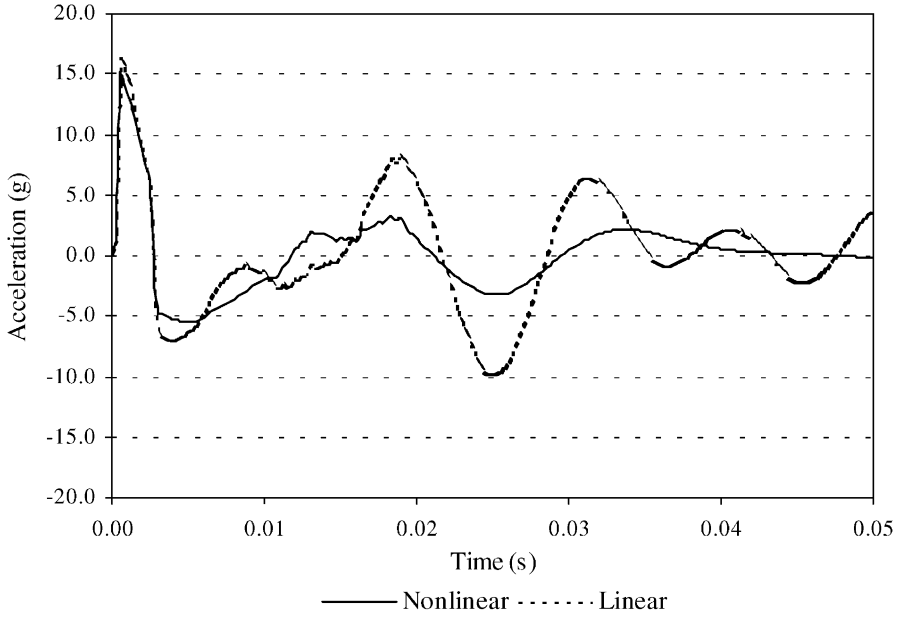

(a) Position 1

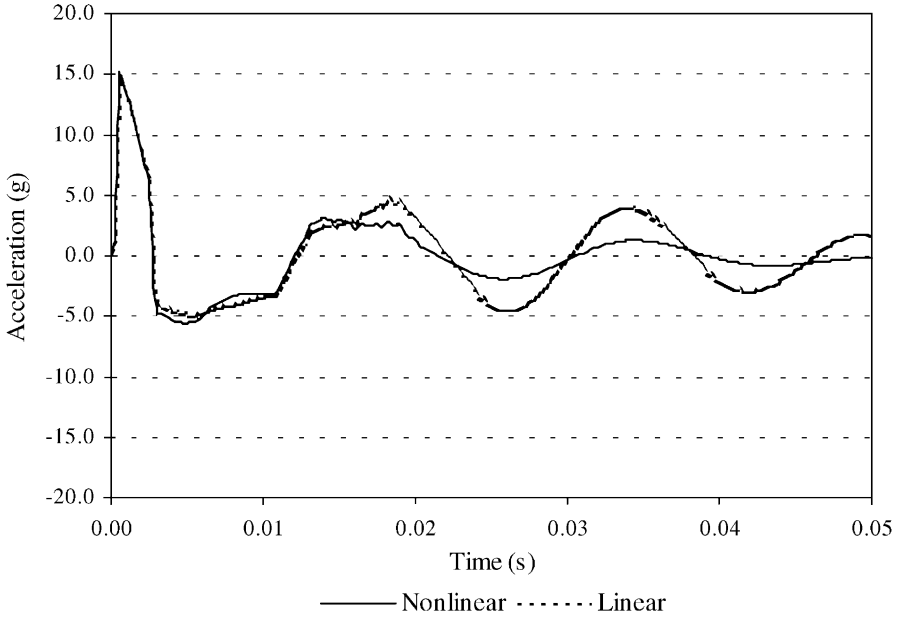

(b) Position 2

Fig. 9. Numerical linear and nonlinear geometric response. Plate A.

for the case of Test 1. For the case of Tests 2 and 4 it was necessary to include more modes in the model and 60 modes were considered.

On the other hand, an analysis using the direct integration method was carried out in order to verify if the effect of geometric nonlinearity due to large displacement was important in the response. In this type of analysis, the elements are formulated in the actual configuration (Eulerian formulation) and the distortion from its original forms during the calculation is kept in mind. In Fig. 9, a comparison of results is shown when linear and nonlinear geometric behavior have been considered. The responses obtained show a similar response in the forced vibration zone. In the free vibration zone, the similarity between them is acceptable. Then, both analyses lead to similar results and it is not necessary, in this case, considering the geometric nonlinear effects.

3.2. Metallic plate clamped in the four edges (Plate B)

Model 1 of Plate B is formed by 100 elements (10×10 mesh). A mesh of 400 elements (20×20 elements) was used as *Model 2* to study the influence of the refinement of the mesh in the results.

The damping coefficient, experimentally determined as indicated in 2.4, was 2.2%.

3.2.1. External action

As in the case of plate A, initially, the response of the plate was determined utilizing as external action the shock wave shown in Fig. 7. On the other hand, as a simpler theoretical proposal, the external pressure due to a shock wave is presented in Fig. 10. This theoretical external load, applicable to thin structures, can be useful as a first approximation for predictions in the design stage.

The scaled distance is defined by

$$Z = \frac{R}{W^{1/3}} \tag{1}$$

in which R is the real distance from an explosive charge W.

The peak overpressure p_s and the duration of the positive phase t_s are determined as a function of the weight of the explosive load W and the scaled distance Z, using charts or equations. For example, the equations given by Kinney and Graham [19] are

$$\frac{p_s}{p_0} = \frac{808\left(1 + \left(\frac{Z}{4.5}\right)^2\right)}{\sqrt{1 + \left(\frac{Z}{0.048}\right)^2}\sqrt{1 + \left(\frac{Z}{0.32}\right)^2}\sqrt{1 + \left(\frac{Z}{1.35}\right)^2}}, \tag{2}$$

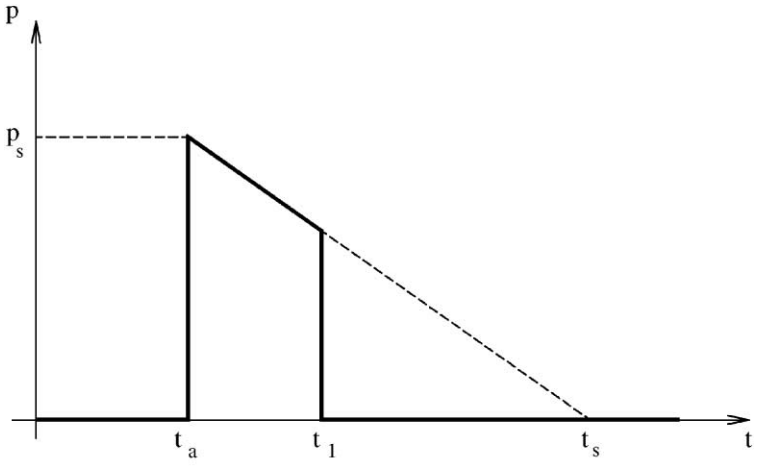

(a) Load proposed

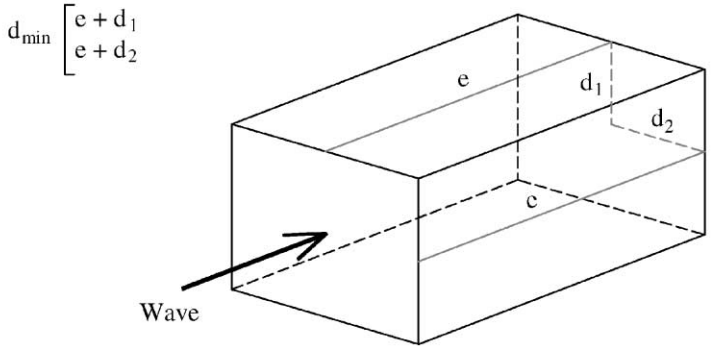

(b) Distances considered

Fig. 10. External load proposed.

$$\frac{t_s}{W^{1/3}} = \frac{980\left[1+\left(\frac{Z}{0.54}\right)^{10}\right]}{\left[1+\left(\frac{Z}{0.02}\right)^{3}\right]\left[1+\left(\frac{Z}{0.74}\right)^{6}\right]\sqrt{1+\left(\frac{Z}{6.9}\right)^{2}}}, \tag{3}$$

in which p_0 is the atmospheric pressure.

On the other hand, the cut time t_1 (Fig. 10) is determined from:

$$t_1 = \frac{d_{\min}}{V_s}, \tag{4}$$

in which $d_{\min}$ is the minimum distance to the center of the back face of the structure according to Fig. 10 and V_s is the velocity of the shock wave determined theoretically or experimentally. For

Table 2
Parameters of the blast waves for all tests

Test	Z (m/kg$^{1/3}$)	p_s (kPa)	t_s (ms)	V_s (m/s)	d_{min} (m)	t_1 (ms)
1	49.9	1.3	6.0	342	0.475	1.5
2	27.8	2.5	11.6	344	0.475	1.5
3	55.0	1.2	6.5	342	0.475	1.5
4	13.9	6.1	10.1	349	0.475	1.4

example, Smith and Hetherington [2] present

$$V_s = \sqrt{\frac{6p_s + 7p_0}{7p_0}}\, a_0, \tag{5}$$

in which a_0 is the speed of sound in air.

The parameters of the blast waves for all tests corresponding to the position of sensor 1 are listed in Table 2.

The proposed $p(t)$ should be used for thin structures for which $t_1 \leqslant t_s$, or, using (3), (4) and (5):

$$d_{min} \leqslant \frac{980\left[1 + \left(\frac{Z}{0.54}\right)^{10}\right]}{\left[1 + \left(\frac{Z}{0.02}\right)^{3}\right]\left[1 + \left(\frac{Z}{0.74}\right)^{6}\right]\sqrt{1 + \left(\frac{Z}{6.9}\right)^{2}}} \sqrt{\frac{6p_s + 7p_0}{7p_0}}\, W^{1/3} a_0. \tag{6}$$

3.2.2. Dynamic response

The acceleration in the center of the plate was determined using the modal superposition method with 16 and 20 modes and the response is shown in Fig. 11 for Test 1. An important difference in the initial value of acceleration was observed as a function of the quantity of modes that were considered in the analysis. This fact indicated clearly that an important issue in the computational analysis of structures under the action of impulsive loads is to select appropriately the quantity of modes to represent appropriately the dynamic behavior of the analyzed structure. On the other hand, the responses to Models 1 and 2 are presented in Fig. 12.

4. Comparison and discussion

In view of the objectives of the paper, a comparison between the computational and the experimental results of the time-history of the accelerations is carried out at this point. For the purpose of comparison, Model 2 (refined) was used in all the cases.

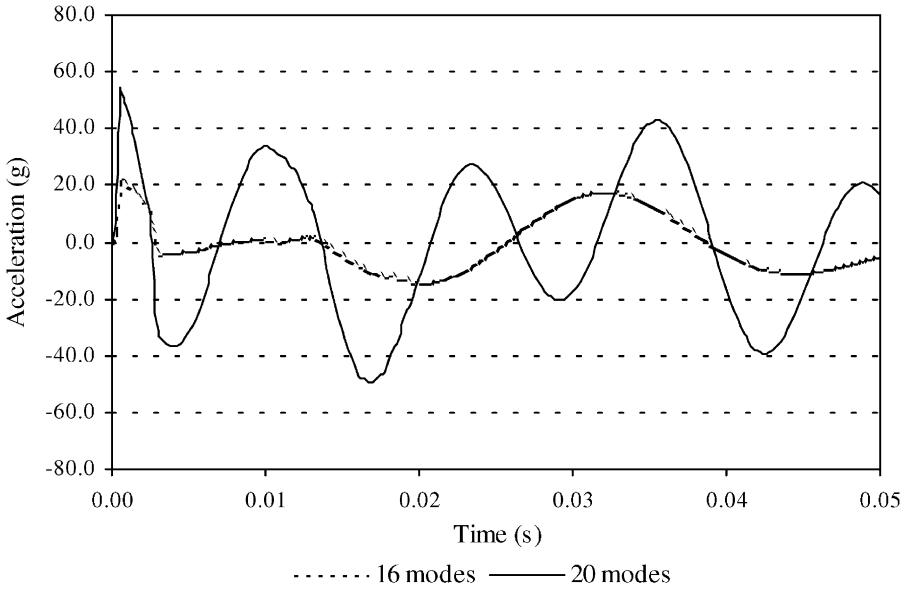

Fig. 11. Numerical response with 16 and 20 modes. Plate B.

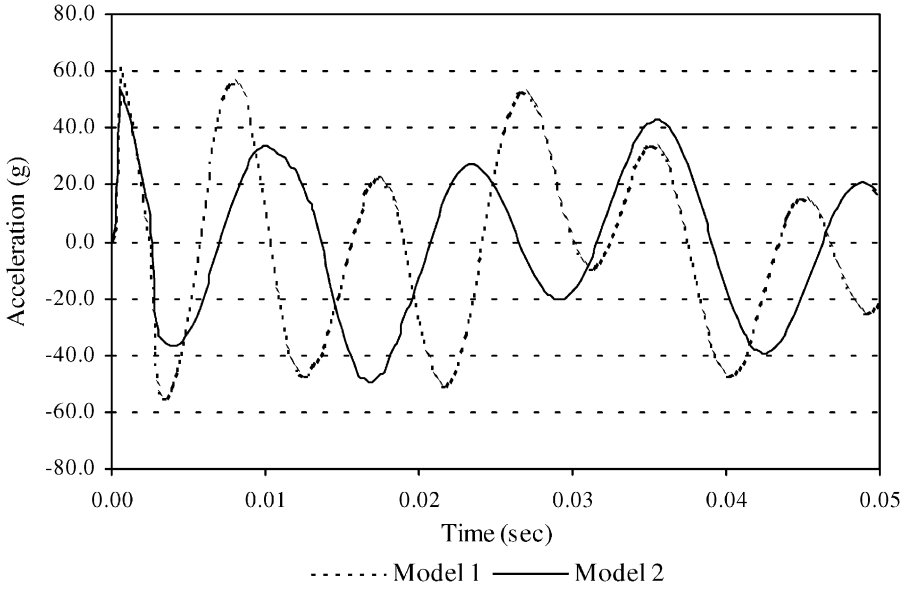

Fig. 12. Numerical response. Plate B.

4.1. Plate A

In Figs. 13–15, the experimental values of the time history of the acceleration of Plate A are compared with those obtained using the ABAQUS program for Tests 1, 2 and 4, respectively.

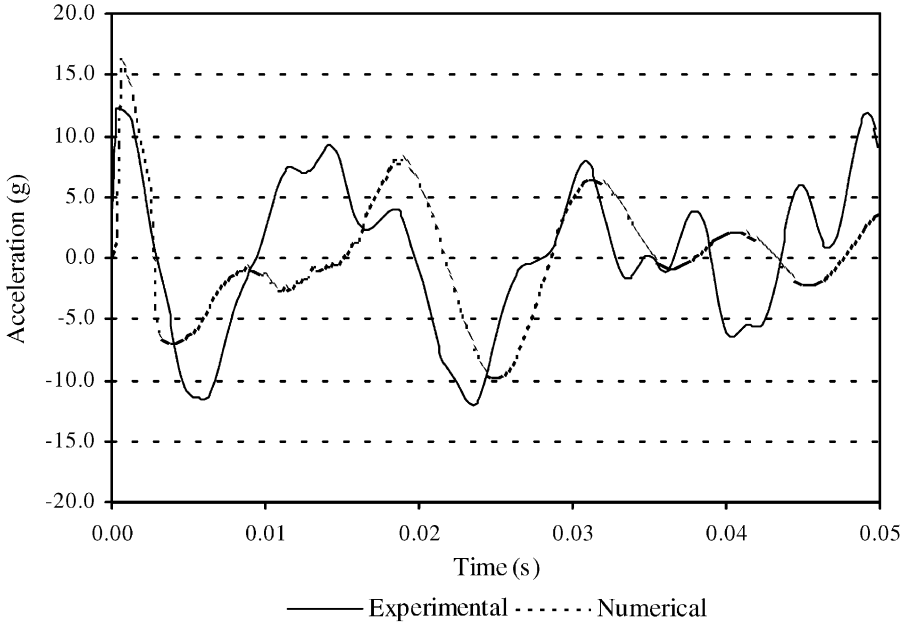

(a) Position 1

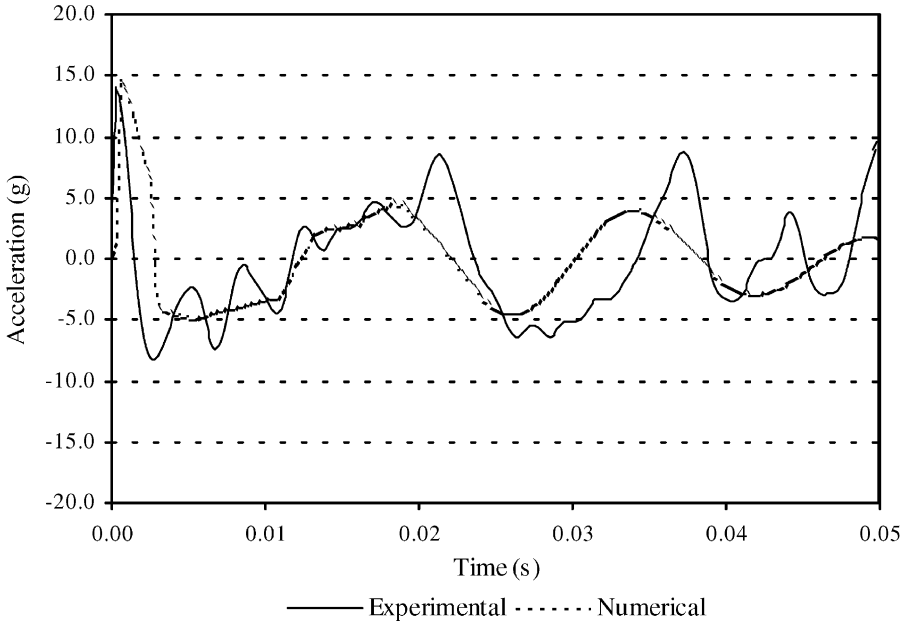

(b) Position 2

Fig. 13. Comparison of experimental and numerical responses. Plate A. Test 1.

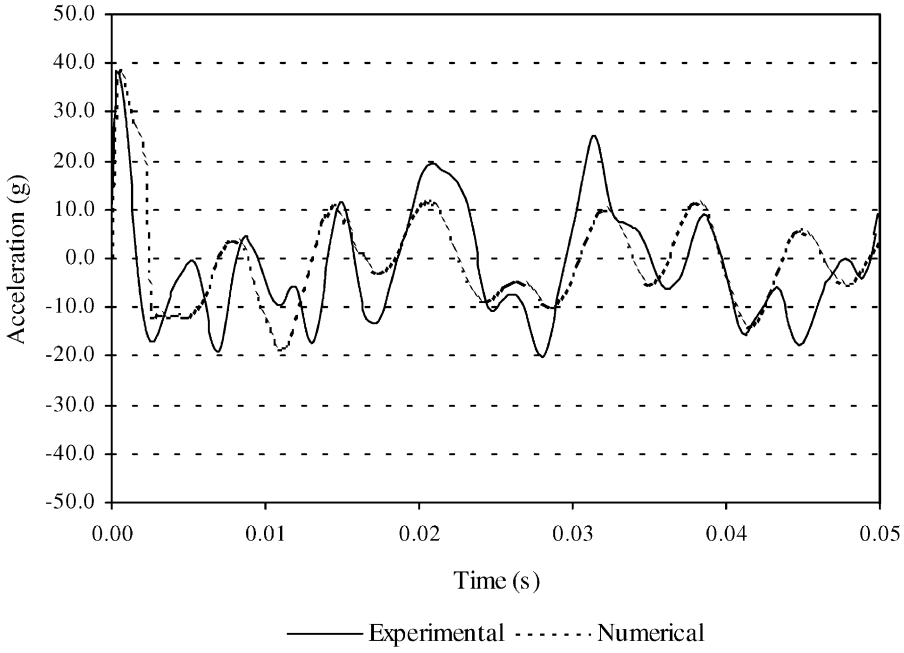

(a) Position 2

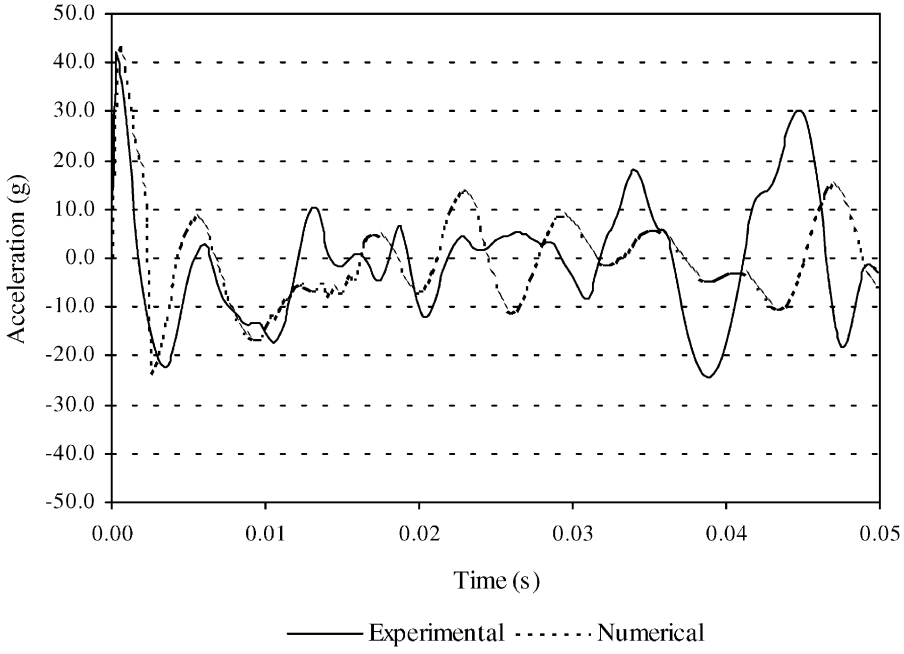

(b) Position 3

Fig. 14. Comparison of experimental and numerical responses. Plate A. Test 2.

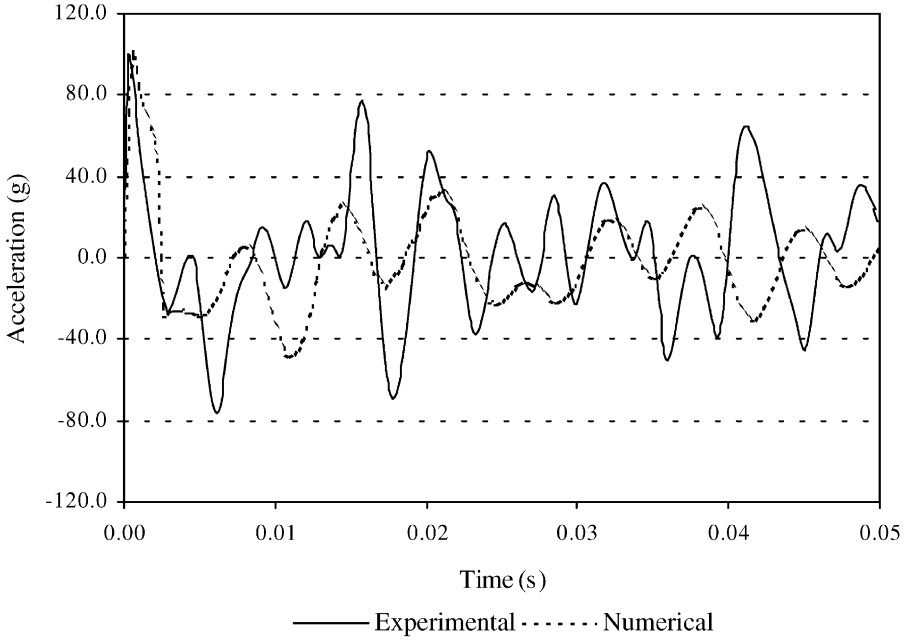

(a) Position 2

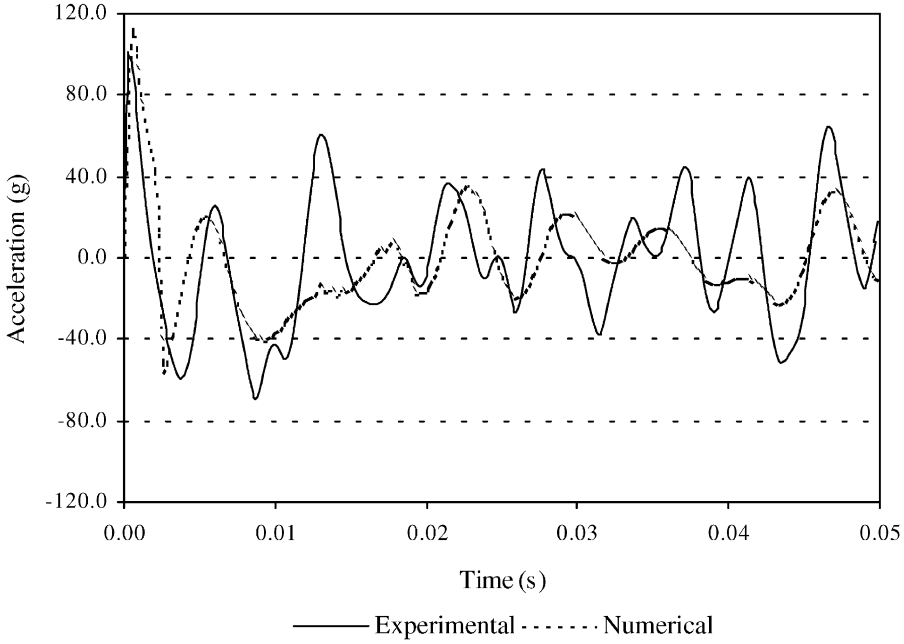

(b) Position 3

Fig. 15. Comparison of experimental and numerical responses. Plate A. Test 4.

Table 3
Peak acceleration (g). Plate A

Position	Test 1			Test 2			Test 4		
	Measured	Numerical	Diff. (%)	Measured	Numerical	Diff. (%)	Measured	Numerical	Diff. (%)
1	12.28	16.28	32.6	39.21	38.59	1.6	—	—	—
2	13.89	14.49	4.3	38.42	38.92	1.3	99.40	99.80	0.4
3	—	—	—	41.88	43.35	3.5	100.01	111.52	11.5

These results were obtained using the modal superposition method considering 30 modes for Test 1 and 60 modes for Tests 2 and 4. It is important to note that the response is shown for a long time (50 ms), that is, approximately 2.5 times the duration of the external load.

For Test 1, in the case of position 1, the peak of the positive phase is overestimated and the peak of the negative phase is underestimated. The differences could be due to the fact that the front of the shock wave is not as plane as it was supposed in the numerical analysis. In the case of position 2, an adequate adjustment was achieved in the forced vibration zone. In the free vibration zone, there was not a complete coincidence for high frequencies. For Test 2, it can be observed that excellent adjustment was made in the case of positions 2 and 3. For Test 4, a very good prediction is found for the forced vibration zone and the peaks of the free vibration zone are underestimated.

Finally, in Table 3 the peak values of acceleration in positions 1–3 of Plate A are compared. It can be observed again that a very good adjustment was achieved in the values except for test 1, position 1 for the reasons explained above.

4.2. Plate B. Test 1

In Fig. 16, the experimental values of the time history of the acceleration of Plate B are compared with those obtained using the ABAQUS program when 20 modal forms are considered. In Fig. 17, the experimental response with the numerical one are compared again, but the external load used in this case is the simpler external pressure proposed in Section 3.2.1. In Table 4, the differences between the experimental and numerical peak values of accelerations are shown, when 16 and 20 modal forms were considered. It can be concluded that a good prediction of the peak values of acceleration was obtained when 20 modal forms were used. It should be noted that, for the case of Plate B, only the response of Test 1 was measured because of the large accelerations involved.

The results obtained show that in both cases there were good predictions in the forced zone of the load although the proposed load present a better adjustment of the peak acceleration (see Table 4). In the free vibration zone, the proposed load did not have a complete coincidence for high frequencies and the peak values were lesser than that obtained with the measured load, which present a much better adjustment. For both cases, the measured damping was applied in the numerical analysis. As the proposed load does not have the negative part of the real pressures, the response in Fig. 17 is apparently more damped.

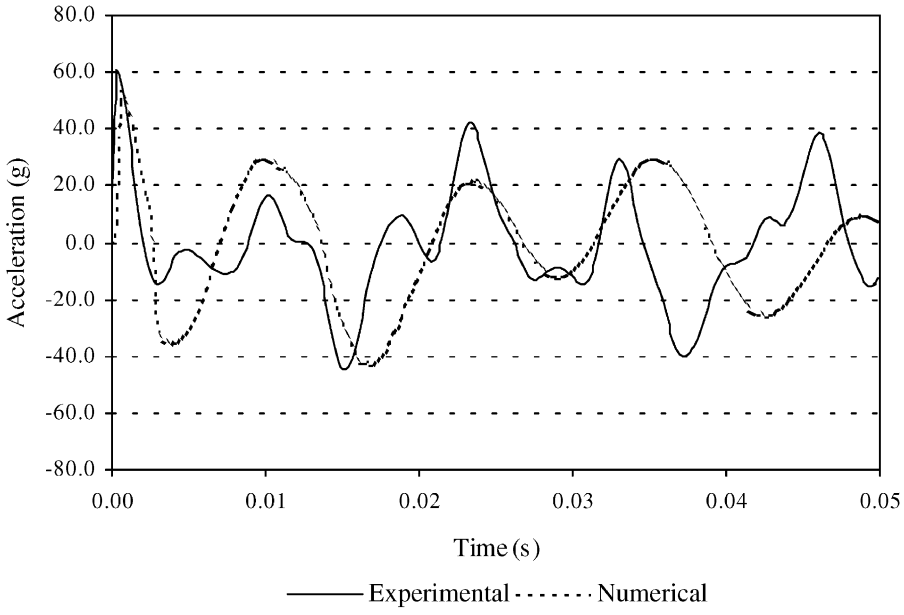

Fig. 16. Comparison of experimental and numerical responses. Plate B. External measured load.

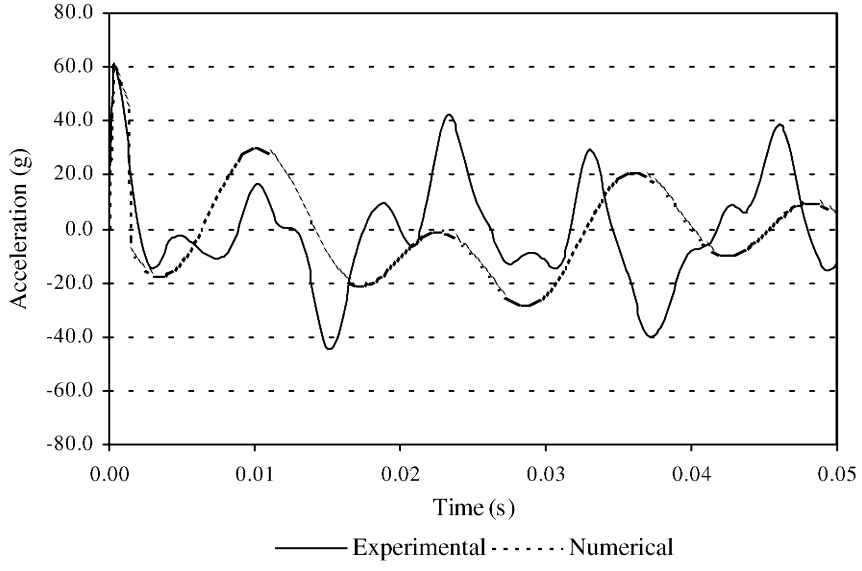

Fig. 17. Comparison of experimental and numerical responses. Plate B. External proposed load.

5. Conclusions

A set of experimental results of unstiffened steel plates subjected to blast load is presented. Moreover, for comparison purposes, a numerical analysis was carried out. On the basis of the

Table 4
Peak acceleration (g). Plate B

Experimental	Numerical					
	External load measured				External load proposed	
	16 modes	Diff. (%)	20 modes	Diff. (%)	20 modes	Diff. (%)
61.08	21.90	64.15	53.25	12.82	60.73	0.57

results obtained, the following conclusions may be drawn:

1. According to Fig. 11 and Table 4, it is extremely important that the number of vibration modes be considered in the analysis because, in general, this type of loads excites the high frequencies. Then, for predicting numerical analysis, it is necessary to carry out numerical tests in order to determine the appropriate quantity of modes that will be used in the numerical analysis.
2. The element size of computational models should agree with the quantity of modes that will be included in the response. As more refined meshes capture the high frequencies with minor errors (see Figs. 8 and 12) and these frequencies have a significant participation in the obtained response, it is very important to determine its values accurately.
3. The obtained results improved significantly when the used load was considered as the temporal superposition of the pressure over the anterior and posterior faces of the plates. However, the difference in the initial value of acceleration in the top of Plate A (free) indicates that the expression of the load applied over this type of contours should be improved.
4. According to Figs. 16 and 17, for prediction purposes of thin structures, it is enough to use the simpler external pressure proposed in Fig. 10.

Acknowledgements

The authors wishes to thank the collaboration of Eng. Sergio Salomón the owner of the test field and the help received from technical staff, Mr. Eduardo Batalla and Mr. Daniel Torielli, during the development and preparation of the tests. Moreover, the financial support of the CONICET and the Universidad Nacional de Tucumán is also gratefully acknowledged. Special acknowledgements are extended to one of the reviewers of the first version of the paper, since his useful suggestions led to many improvements of the work.

References

[1] Baker WE, Cox PA, Westine PS, Kulesz JJ, Strehlow RA. Explosion hazards and evaluation. Amsterdam: Elsevier, 1983.
[2] Smith PD, Hetherington JG. Blast and ballistic loading of structures. Great Britain: Butterworth-Heinemann Ltd., 1994.
[3] Biggs JM. Introduction to structural dynamics. New York: McGraw-Hill, 1964.

[4] Clough RW, Penzien J. Dynamics of structures. New York: McGraw Hill, Inc., 1975.
[5] Autoridad Regulatoria Nuclear. Efecto de Explosionesy Acciones Mitigantes Aplicables a Estructuras, Sistemas y Componentes de Instalaciones Civiles. 10 al 14 de Agosto de 1998, Buenos Aires, Argentina.
[6] Galiev U. Experimental observations and discussion of counterintuitive behavior of plates and shallow shells subjected to blast loading. Int J Impact Eng 1996;18(7–8):783–802.
[7] Krauthammer T, Ku CK. A hybrid computational approach for the analysis of blast resistant connections. Comput Struct 1996;61(5):831–43.
[8] Louca LA, Pan YG. Response of stiffened and unstiffened plates subjected to blast loading. Eng Struct 1998;20(12):1079–86.
[9] Ellis BR, Tsui F. Testing and analysis of reinforced concrete panels subjects to explosive and static loading. Proc Inst Civ Eng Struct Bldg 1997;122:293–304.
[10] Jones N. Plastic failure of ductile beams loaded dynamically. J Eng Ind Trans ASME 1976;98:131–6.
[11] Nonaka T. Shear failure of a steel member due to a blast. Int J Impact Eng 2000;24(3):231–8.
[12] Formby SA, Wharton RK. Blast characteristics and TNT equivalence values for some commercial explosives detonated at ground level. J Hazard Mater 1996;50:183–98.
[13] ABAQUS/Standard 5.7-3. User's Manual, 1997.
[14] Rudrapatna NS, Vaziri R, Olson MD. Deformation and failure of blast-loaded stiffened plates. Int J Impact Eng 2000;24:457–74.
[15] Shen WQ, Jones N. Dynamic response and failure of fully clamped circular plates under impulsive loading. Int J Impact Eng 1993;13:259–78.
[16] Pan YG, Louca LA. Experimental and numerical studies on the response of stiffened plates subjected to gas explosions. J Construct Steel Res 1999;52:171–93.
[17] NUREG/CR-6190. Protection against malevolent use of vehicles at nuclear power plants. US Nuclear Regulatory Commission. Vol. 2. August 1994.
[18] Woodhouse J. Linear damping models for structural vibration. J Sound Vib 1998;215(3):547–69.
[19] Kinney GF, Graham KJ. Explosive shocks in air, 2nd ed. Berlin: Springer, 1985.